

EUROPEAN COOPERATION  
IN THE FIELD OF SCIENTIFIC  
AND TECHNICAL RESEARCH

---

COST 273 TD(03) 099  
Paris, France  
2003/May/22-23

---

EURO-COST

---

SOURCE: Unité Electronique et Informatique (UEI),  
Ecole Nationale Supérieure des Techniques Avancées (ENSTA),  
France

## **MIMO Channel Capacity and Mutual Coupling in Circular Arrays of Monopoles**

Van Phuong TRAN and Alain SIBILLE  
Ecole Nationale Supérieure des Techniques Avancées (ENSTA)  
32 Boulevard Victor  
75739 Paris Cedex 15  
FRANCE  
Phone: + 33-1-45 52 54 34  
Fax: + 33-1-45 52 83 27  
Email: [tran@ensta.fr](mailto:tran@ensta.fr), [sibille@ensta.fr](mailto:sibille@ensta.fr)

# **MIMO Channel Capacity and Mutual Coupling in Circular Arrays of Monopoles**

Van Phuong TRAN and Alain SIBILLE

ENSTA, 32 Boulevard Victor, 75739 Paris Cedex 15, France

## **Abstract :**

The role of electromagnetic inter-sensor coupling on the capacity of MIMO channels is investigated, in the case of circular arrays of monopoles. Both real arrays and artificial arrays with partially or totally suppressed coupling are compared, in order to understand the phenomena involved in the enhancement or the reduction of the capacity by coupling. The analysis performed in this paper allows to separate the contributions of correlation of wave fields due to spatial variance, from that of coupled currents in the monopoles, or from array directivity, or from phase distortion.

## **I – Introduction :**

The use of Multi-Element Antennas (MEA) in wireless communications led to considerable research because of high achievable data rates. Indeed, this type of antenna allows the multipath effects of the radiomobile channel to be mitigated or even to be usefully exploited. It is shown that communication systems with MEA at both ends of links (Multiple-Input Multiple-Output : MIMO systems), have good performances in rich multipath environment [1]. Its principle consists in taking advantage of the multipath character in order to decompose the channel as several independent parallel subchannels. Thereby, high channel capacities are implemented. To take the best advantages of MIMO systems, the element antennas need to be sufficiently spaced in the arrays. But large size antennas cannot be installed on mobile stations. The correlation between signals indeed increases if the inter-sensor distance decreases, and the channel capacity is expected to be reduced with increasing correlation. In addition, the existence of mutual coupling has to be taken account for small size arrays, and it can affect MIMO performances. In the present paper, we first introduce the channel model used in simulations and describe the various antenna arrays we consider in order to evaluate the influence of mutual coupling. Certain array types are already introduced in a previous work to separate the contributions of spatial correlation and of mutual coupling [2]. Then we discuss the simulated channel capacities using these array configurations, based on the analysis of the mutual impedances between elements and of the complex radiated fields. Finally, we conclude about the effects of mutual coupling on MIMO communication systems.

## **II – System Model :**

We consider a wireless communication system with  $n_T$  elements antennas at the transmitter side and  $n_R$  elements antennas at the receiver side (Fig. 1). Each element antenna is loaded by a real impedance  $Z_L$ . Here,  $X(n_T)$  and  $Y(n_R)$  are the transmitted signals vector and the received signals vector respectively. These two vectors can be linked by :

$$Y(n_R) = H(n_R, n_T)X(n_T) + N(n_R)$$

$H(n_R, n_T)$  is the channel matrix characterizing the system. Each element  $H_{ij}$  of  $H(n_R, n_T)$  is the complex transmission coefficient between the transmit antenna  $j$  to the receive antenna  $i$ .  $H(n_R, n_T)$  links the picked up voltages  $Y_i$  on each load  $Z_L$  at the receiver side to the emf  $X_i$  applied to each antenna at the transmitter side.  $N(n_R)$  is an added noise vector.

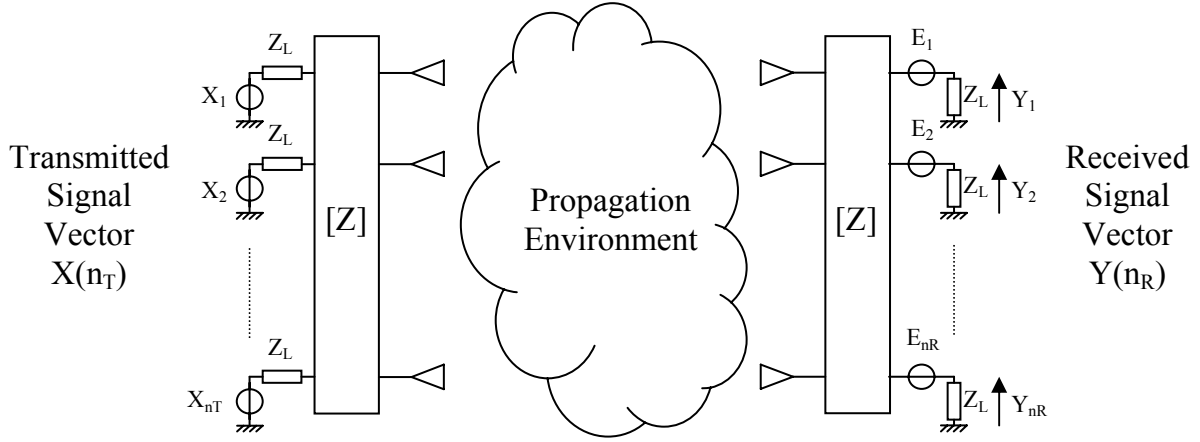


Fig. 1. MIMO system with mutual coupling

The matrices  $Z(n_T, n_T)$  at the transmitter side and  $Z(n_R, n_R)$  at the receiver side represent the existing inter-sensor coupling between the element antennas. If there is no mutual coupling, the channel matrix  $H(n_R, n_T)$  can be decomposed as :

$$H(n_R, n_T) = A_R(n_R, N)W(N, M)A_T^T(n_T, M)$$

The superscript  $T$  designates the transposition operation.  $W(N, M)$  is called the Wave Connecting Matrix (WCM).  $M$  and  $N$  are the number of transmitted and received waves respectively. This type of matrix is in particular used to model keyholes (one transmitted/received wave can correspond to more than one received/transmitted wave) [3]. In the present paper, it models the propagation environment and links the arrival waves to the departure waves by complex coefficients. A rich multipath environment can be obtained with e.g. 10 waves, and a pure diagonal matrix with unity or Rayleigh distributed entries on the diagonal.  $A_T(n_T, M)$  and  $A_R(n_R, M)$  are two steering matrices relating the propagating waves to the transmitted or received signals. In the presence of mutual coupling, the matrices  $A_T(n_T, M)$  and  $A_R(n_R, N)$  are replaced by the complex gain matrices  $G_T(n_T, M)$  and  $G_R(n_R, N)$  :

$$H(n_R, n_T) = G_R(n_R, N)W(N, M)G_T^T(n_T, M)$$

The channel capacity is calculated by this well-known formula [4] :

$$C = \log_2 \left[ \det \left( I_{n_R} + \frac{\rho}{n_T} HH^H \right) \right]$$

Where  $I_{n_R}$  returns the  $n_R \times n_R$  identity matrix.  $\rho$  is the Signal to Noise Ratio (SNR) and will be kept to 20 dB. The superscript  $H$  designates the conjugate transposition operation. The channel matrix  $H(n_R, n_T)$  will be normalized as the following condition :

$$\|H(n_R, n_T)\|_F^2 = n_R n_T$$

$\|H(n_R, n_T)\|_F$  is the Frobenius norm of the matrix  $H(n_R, n_T)$ . This condition allows antenna gains to enter the channel capacity. The Directions Of Departure (DOD) and the Directions Of Arrival (DOA) will be chosen randomly over an omnidirectional azimuth scenario. To complete the statistical distribution of channel realizations, a small-scale statistic is introduced by varying the whole antennas positions on a grid with  $\lambda$  or  $2\lambda$  side lengths in the horizontal plane,  $\lambda$  being the wavelength. Thereby, the channel capacity  $C$  in b/s/Hz is also a random variable. Its Cumulative Density Function (CDF) will be computed. And to determine the performance of the MIMO systems, we will refer to the mean value of the capacity  $C$ .

### III – Array Antenna Configurations :

Let us consider different circular arrays of monopoles which are defined by the array diameter  $d$ , the number of sensors  $n$  and the load impedance  $Z_L$  :

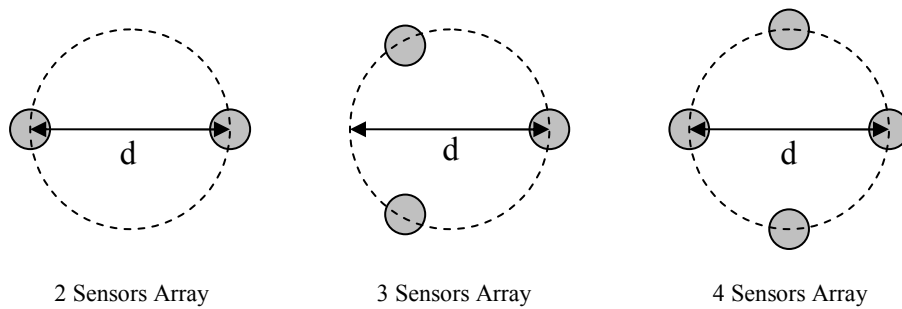


Fig. 2. Circular array topologies

For an array of  $n$  sensors, a number of  $n$  complex radiation patterns is calculated by exciting only one element under a voltage of 1V at a given time, the others being loaded. All patterns are obtained from the complex radiated field by a single isolated monopole at the frequency 4.74 GHz. The length of the monopole is 15 mm corresponding to a theoretical resonance frequency 5 GHz. In practice, the resonance frequency is equal to 4.74 GHz due to the monopole thickness (0.1 mm).

#### III-1 – Real Array :

We first introduce a real array where mutual coupling is included. To obtain each radiated field by each element antenna, we compute the matrix  $Z(n, n)$  of the array of a diameter  $d_C$  and we calculate the induced currents vector  $I(n)$  by solving this matrix equation :

$$E(n) = [Z(n, n) + \text{diag}_n(Z_L)].I(n)$$

$E(n)$  is the excitation voltages vector where the element  $E_i$  is equal to 1V and the others to 0V.  $i$  being the index of the excited port.  $\text{diag}_n(Z_L)$  returns a  $n \times n$  diagonal matrix where the diagonal elements are equal to  $Z_L$ . Although it is possible to compute directly the complex radiation patterns of the full array, another possibility is to apply the excitation currents  $I_1$  to  $I_n$  to a virtual array of a diameter  $d_S$  equal to  $d_C$  ( $d_S = d_C = d$ ) which is describe in the next subsection (Fig. 3). This is only approximate, however we checked that the computed patterns reproduce the true ones very closely.

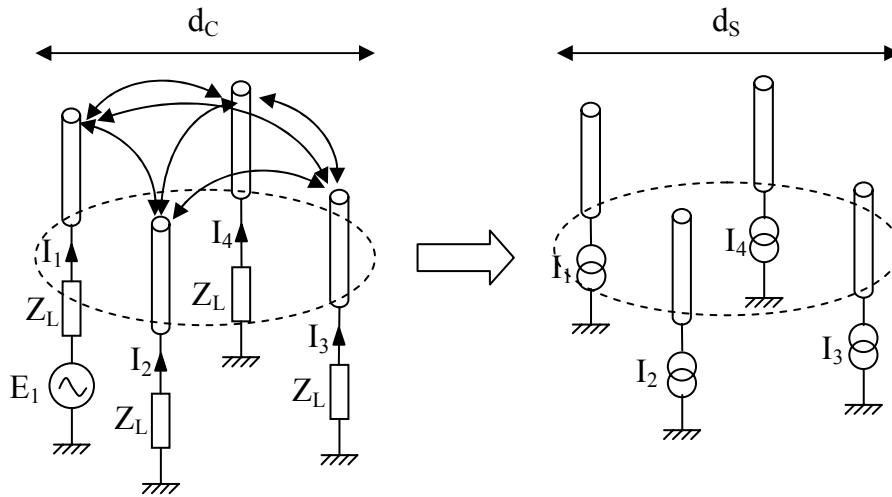


Fig. 3. Real array (left) and modelling approach (right)

### III-2 – Virtual Array :

In a virtual array, mutual coupling is trivially absent. To obtain the  $n$  radiation patterns of this type of array, we duplicate the pattern of the single monopole at  $n$  different positions taking account the steering vectors (Fig. 4).

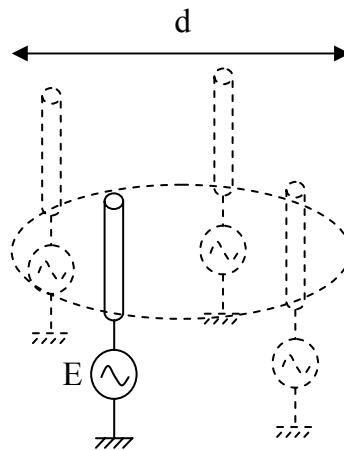


Fig. 4. Virtual array

### III-3 – Arrays with artificially modified spatial correlation or coupling :

To dissociate the contribution of antennas spacing and of mutual coupling, we will also simulate MIMO channels with artificially modified correlation/coupling arrays where  $d_C \neq d_S$  (see Fig. 3). Thereby, they cannot be called real arrays anymore. To put emphasis on spatial correlation, we will investigate many arrays where  $d_S$  is low and  $d_C$  is high. If  $d_S$  is high and  $d_C$  is low alternatively, the effect of mutual coupling will be investigated. We will see later that  $d_S$  does not necessarily have to take a very large value for small spatial correlations to be achieved. We can notice that a virtual array can be obtained with a very high value of  $d_C$ . The real array and the virtual array are two particular cases of this array type.

### III-4 – Arrays with artificial radiation patterns :

The radiation patterns are complex. To place emphasis on the contributions of the magnitude or alternatively of the phase of the patterns, we will simulate channel capacity with two other types of arrays, where patterns are based on the real array or on the virtual array. If we denote the radiated fields by the element antenna  $i$  of a real array and of a virtual array :

$$E_{Ri}(\varphi, \theta) = \rho_{Ri}(\varphi, \theta) \exp[j\psi_{Ri}(\varphi, \theta)] \text{ and } E_{Vi}(\varphi, \theta) = \rho_{Vi}(\varphi, \theta) \exp[j\psi_{Vi}(\varphi, \theta)]$$

Where  $E_{Ri}(\varphi, \theta)$  and  $E_{Vi}(\varphi, \theta)$  are the complex radiated fields by an element antenna of a real array and of a virtual array respectively.  $\rho_{Ri}(\varphi, \theta)$  and  $\rho_{Vi}(\varphi, \theta)$  are the magnitudes of the radiated fields.  $\psi_{Ri}(\varphi, \theta)$  and  $\psi_{Vi}(\varphi, \theta)$  are the phases.  $\varphi$  is the azimuth angle.  $\theta$  is the elevation angle.  $j$  is the imaginary unit. We will force the radiated fields of two artificial arrays to be as follows :

$$E_{MCI}(\varphi, \theta) = \rho_{Ri}(\varphi, \theta) \exp[j\psi_{Vi}(\varphi, \theta)] \text{ and } E_{PCI}(\varphi, \theta) = \rho_{Vi}(\varphi, \theta) \exp[j\psi_{Ri}(\varphi, \theta)]$$

They will be called Magnitude Coupled Array (MCA) and Phase Coupled Array (PCA). For such arrays, we have  $d_s = d_c$ .

## IV – Simulation Results :

In all simulations presented here, exactly identical MEA arrays are used on the receive and transmit side, whatever the array type. The array complex gain patterns and impedance matrices were in all cases computed “exactly” by a Method Of Moment (MOM) based commercial tool (WIPL).

### IV-1 – Influence of Mutual Coupling :

The MIMO capacity is firstly computed in the case of 2 sensors array in the presence and in the absence of mutual coupling (Real Array and Virtual Array) :

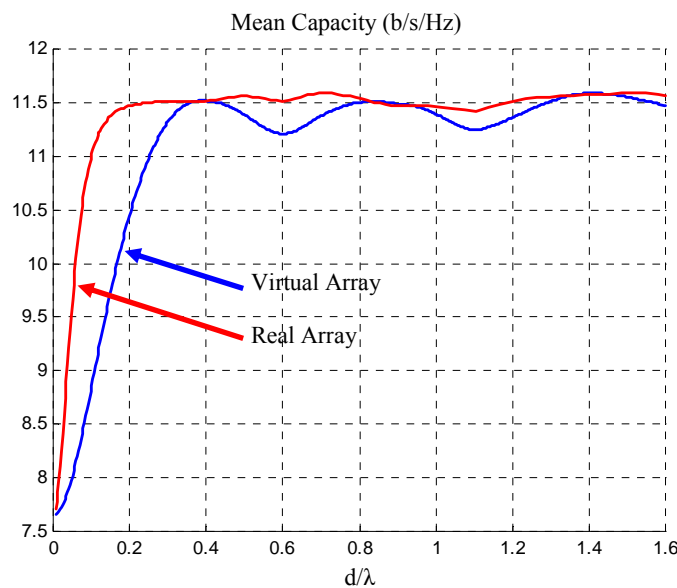


Fig. 5. MIMO capacity with virtual array and real array of 2 sensors

The MIMO capacity with a real array is always greater than or roughly equal to the MIMO capacity with a virtual array, whatever the value of  $d/\lambda$ . As a consequence, mutual coupling has a beneficial effect or no effect at all on the channel capacity. The difference of capacity between the cases of the two array types on one hand, and the mutual impedance  $Z_{21}$  on the other hand are plotted below :

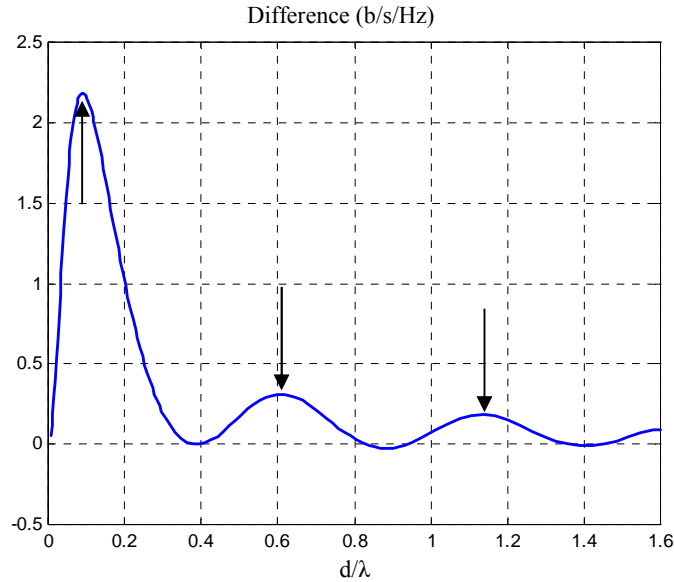


Fig. 6. Difference of MIMO capacity with virtual array and real array of 2 sensors

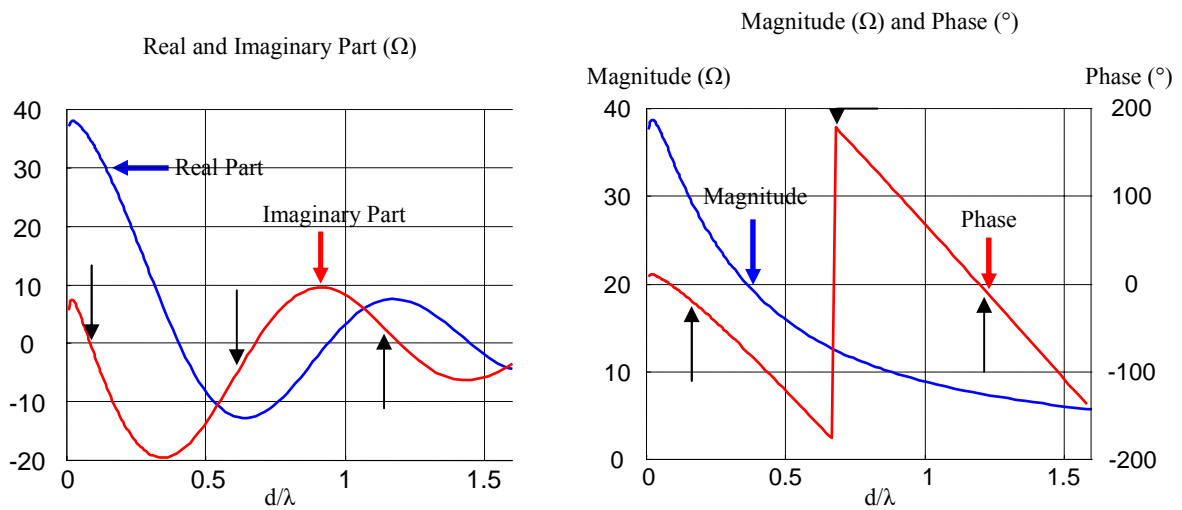


Fig. 7. Mutual impedance  $Z_{21}$  in the case of 2 sensors

We can notice an enhancement of the channel capacity when the mutual impedance  $Z_{21}$  is a real number. On the other hand there is no difference when  $Z_{21}$  is imaginary. The level of the difference is linked to the magnitude of  $Z_{21}$ . This phenomenon is due to a rank deficiency of the channel matrix in the former case, which has been clarified in a previous work [2].

#### IV-2 – Contributions of Antenna Spacing and Mutual Coupling :

In the following simulations (Fig. 8), the element spacing in the arrays is constant for each curve. The matrix  $Z$  used for excitation current calculation only changes. Spatial correlation can be characterized by the Bessel function of the first kind and the zero order  $J_0(2\pi d_s/\lambda)$  [5]. The channel capacity is firstly simulated using 2 sensors arrays where the inter-sensor distance  $d_s = 0.1\lambda$  (strong spatial correlation). And secondly with  $d_s = 0.4\lambda$ . This last value corresponds to a low spatial correlation because it is a zero of the Bessel function.

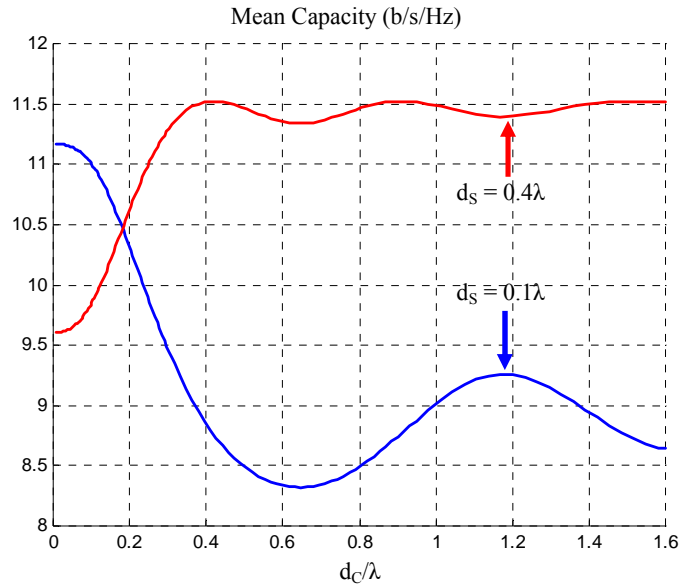


Fig. 8. MIMO capacity with artificially modified coupling arrays

Here,  $d_c/\lambda$  characterizes the introduced mutual coupling by using the matrix  $Z$  at the array diameter  $d_c$  to calculate the excitation currents. When spatial correlation is strong, the mutual coupling is beneficial. Thus, high capacities are obtained at low values of  $d_c/\lambda$  corresponding to strong coupling. The capacity variations appear to coincide with those of the real part of the mutual impedance  $Z_{21}$ . And when spatial correlation can be neglected, mutual coupling decreases the MIMO capacity instead of enhance it as it is shown previously [2]. A decreasing appears when  $Z_{21}$  is a real number.

#### IV-3 – Contributions of the Magnitude and the Phase of Radiated Fields :

The MIMO channel capacity with a real array, a virtual array and arrays with artificial radiation patterns are presented in this following graph :

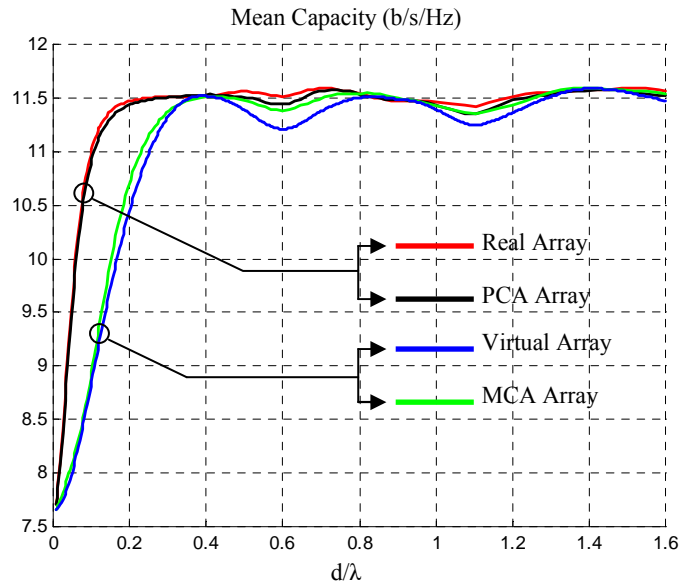


Fig. 9. MIMO capacity with the various array types

The mean capacity with the MCA array is approximately equal to the capacity of the virtual array. And we can say the same thing for the PCA array compared to the real array. In both pairs of arrays, the phases of the radiated fields are common. It thus appears clearly that the phase of radiated fields is more important than their magnitude. We checked that the values of the phases are not important but the difference is significant. We can see below the difference of phase of radiated fields by element antennas of a 2 sensors array where  $d/\lambda = 0.1$  (Maximum of capacity difference) and  $d/\lambda = 0.4$  (Null difference of capacity) :

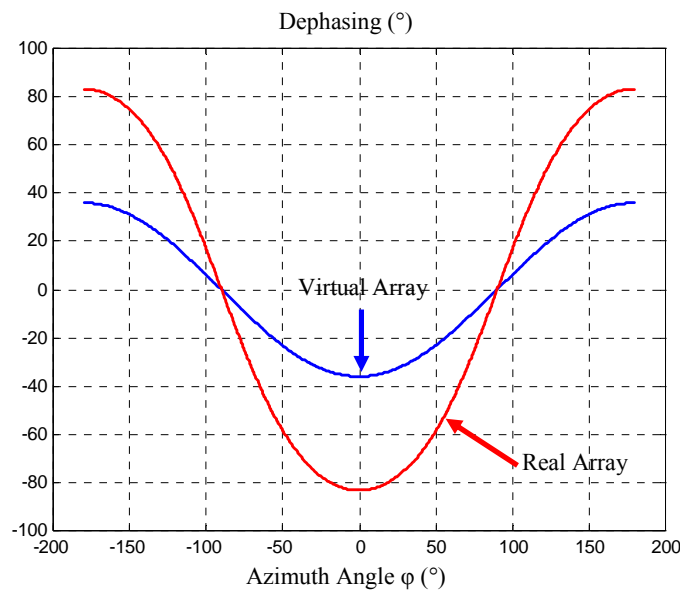


Fig. 10. Dephasing between the radiated fields of both sensors at  $d/\lambda = 0.1$ , for a 2 element array

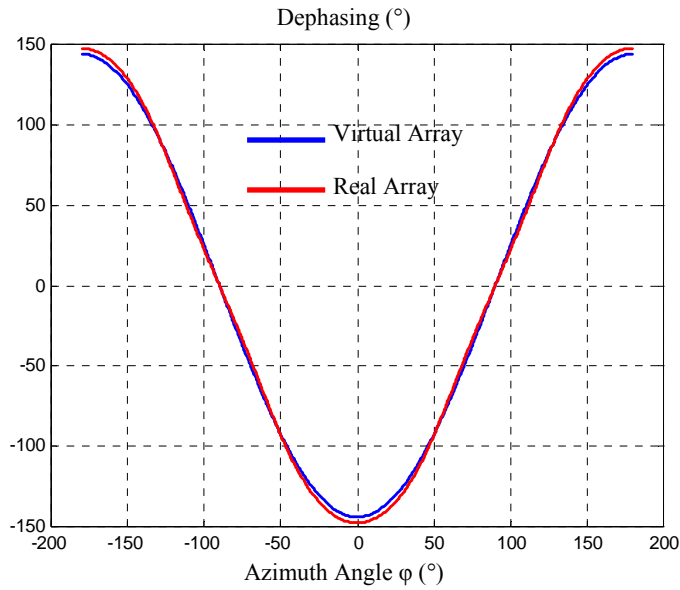


Fig. 11. Dephasing between the radiated fields of both sensors at  $d/\lambda = 0.4$ , for a 2 element array

Where  $d/\lambda = 0.1$ , the dephasing between sensors for the real array is larger than the dephasing for a virtual array. This consequently leads to a higher capacity, as the result of a larger phase diversity. If  $d/\lambda = 0.4$ , the dephasing is the same on the other hand. We can deduce that mutual coupling has no influence on the phases at this array diameter. Thereby, there is no difference of capacity.

We now study the evolution of capacity with the evolution of dephasing in case of virtual array and of real array of 2 sensors :

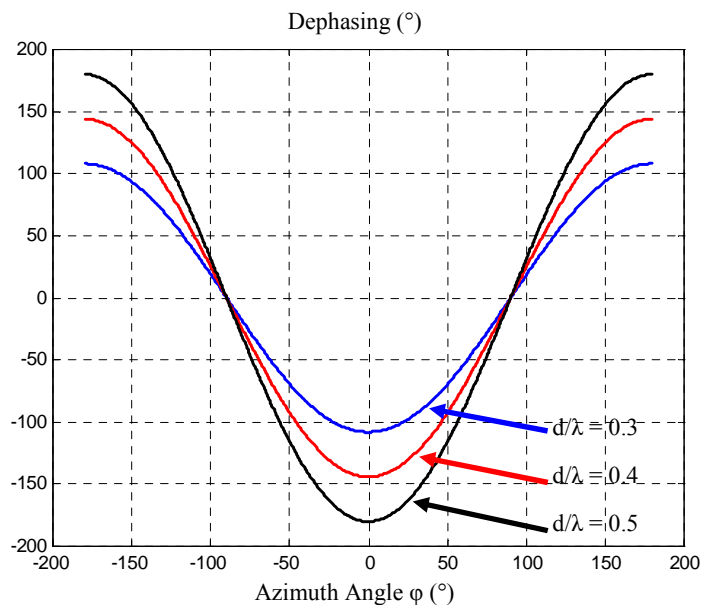


Fig. 12. Dephasing between the radiated fields of both sensors, for a 2 element virtual array

In the case of the virtual array, the dephasing can be written as (in radians) :

$$\xi = 2\pi(d/\lambda)\cos(\varphi)$$

The dephasing can be reduced at a value in range  $[-180^\circ; +180^\circ]$ . We can believe the maximum diversity is obtained for  $d/\lambda = 0.5$  because all possible values of dephasing are swept. But in practice, the channel capacity at  $d/\lambda = 0.5$  is lower than the channel capacity at  $d/\lambda = 0.4$  (which reaches its maximum value). One possible explanation is the dephasing value  $180^\circ$  correspond to the same dephasing as the value  $-180^\circ$ . Thus, the phase diversity is reduced.

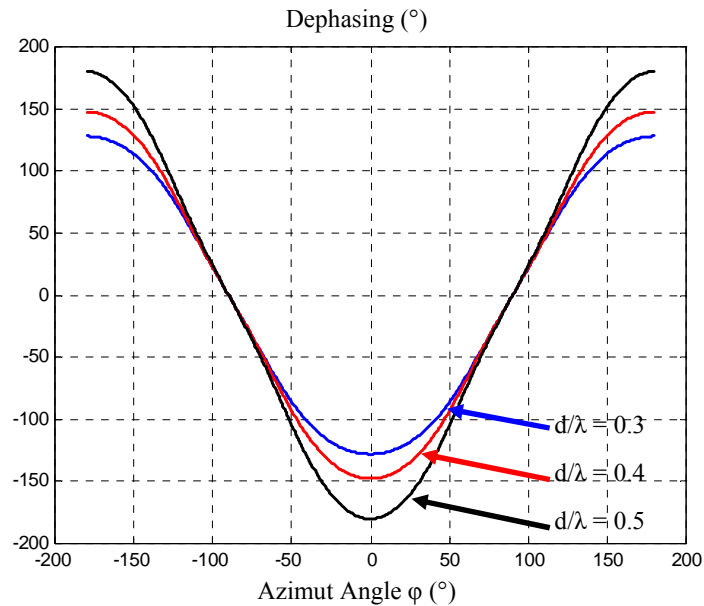


Fig. 13. Dephasing of radiated fields in the case of a 2 sensors real array

In the case of the real array, the three curves correspond approximately to the same channel capacity. Actually it turns out the slopes in azimuth ranges  $[-130^\circ; -50^\circ]$  and  $[50^\circ; 130^\circ]$  are identical. And the dephasing is thus constant everywhere. To realize the best capacity we can hope, the dephasing has to be as much spread as possible. A constant dephasing is useless.

#### IV-4 – Influence of the Number of sensors :

The difference of mean channel capacity between the real array and the virtual array is plotted in the cases of 2, 3 and 4 sensors arrays :

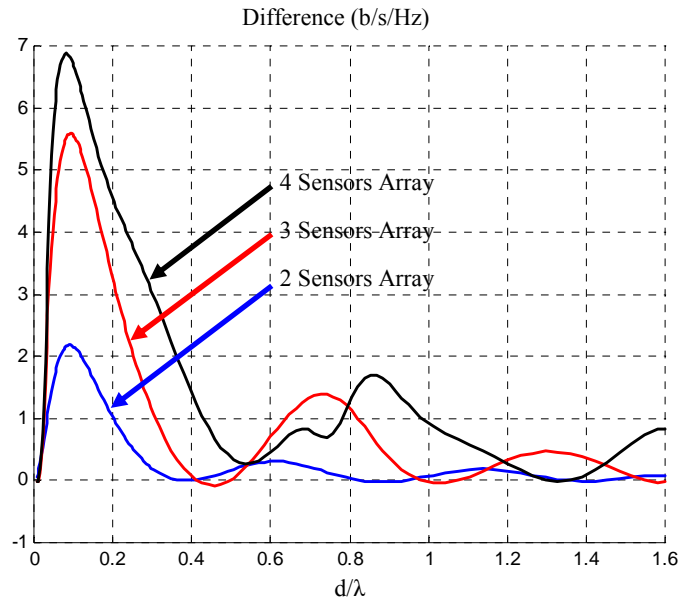


Fig. 14. Difference of MIMO capacity with virtual array and real array of 2, 3 and 4 sensors

In the cases of 3 and 4 sensors, the same capacity enhancements are observed. An enhancement appears when two neighbouring elements are approximately spaced by the same distance where the phenomenon appears in the cases of 2 sensors. In the case of 4 sensors, we can expect twice more enhancement phenomena because two different inter-sensor distances exist due to the array geometry (Fig. 2).

## **V – Conclusion :**

The role of mutual coupling in MIMO antennas in addition to spatial correlation is studied. It is shown that mutual coupling can be beneficial because its presence implies an enhancement of channel capacity in certain cases. Thereby, the optimum antenna size is conveniently reduced. When spatial correlation is strong, mutual coupling enhances the channel capacity. In the absence of spatial correlation, mutual coupling is inconvenient at certain array sizes [2]. We have also seen that MIMO performances were linked to the diversity of the phases, i.e. that the phase behaviour was much more important than the amplitude behaviours as is commonly assumed to explain capacity enhancement due to antenna coupling. However this phase diversity is limited by a range of possible dephasings  $[-180^{\circ}; +180^{\circ}]$ .

## **References :**

- [1] – “MIMO – A Solution for Advanced Wireless Access”, M.A. Beach, D.P. McNamara, P.N. Fletcher and P. Karlsson, 11<sup>th</sup> International Conference on Antennas and Propagation, 17-20 April 2001, Conference Publication No. 480
- [2] – “Inter-Sensor Coupling and Spatial Correlation Effects on the Capacity of Compact MIMO Antennas”, V.P. Tran and A. Sibille, COST 273, 19-20 September 2002, Lisbon (Portugal), Document TD(02) 128
- [3] – “Keyholes and MIMO Channel Modelling”, A. Sibille, COST 273, 15-17 October 2001, Bologna (Italy), Document TD(01) 017

- [4] – “On Limits of Wireless Communications in a Fading Environment when Using Multiple Antennas”, G.J. Foschini and M.J. Gans, *Wireless Personal Communications* 6, pp 311-335, 1998
- [5] – “Microwave Mobile Communications”, W.C. Jakes, IEEE Press, New York, 1994